Synthesis and Stabilization of Nanocrystalline Zirconia with MSU Mesostructure

X. M. Liu,[†,‡] G. Q. Lu,*[,‡] and Z. F. Yan[†,‡]

Key Laboratory for Heavy Oil Processing, Key Laboratory of Catalysis, CNPC, University of Petroleum, Dongying 257061, China, and ARC Centre for Functional Nanomaterials, University of Queensland, QLD 4072, Australia

Received: April 26, 2004; In Final Form: July 25, 2004

In the presence of nonionic block-copolymer surfactant, nanocrystalline zirconia particles with MSU mesostructure were synthesized by a novel solid-state reaction route. The zirconia particles possess a nanocrystalline pore wall, which renders higher thermal stability compared to an amorphous framework. To further enhance its stability, laponite, a synthetic clay, was introduced. Laponite acts as an inhibitor to crystal growth and also as a hard template for the mesostructure. High surface area and ordered pore structure were observed in the stabilized zirconia. The results show that the formation of the MSU structure is attributed to reverse hexagonal micelles, which are the products of the cooperative self-assembly of organic and inorganic species in the solid-state synthesis system with crystalline water and hygroscopic water present.

Introduction

Zirconia is a special transition-metal oxide that possesses bifunctional characteristics of weak acid and base properties.[1,2] The P-type semiconductivity exhibits abundant oxygen vacancies on its surface. The high ion-exchange capacity and redox activities make it possible to be used in many catalytic processes as the catalyst, the supporter, and the promoter. In addition, the superior chemical stability, mechanical strength, and ion-exchange capacity are favorable for applications in ceramic toughening, thermal-barrier coating, electronics, and oxygen sensors.[3−7]

In recent years, many synthesis routes have been proposed for the preparation of mesoporous or nanosized zirconia because of its promising applications. Using a cationic surfactant, Hudson first synthesized mesoporous zirconia with high surface area via a scaffolding mechanism.[8,9] Anionic surfactants have also been used to synthesize mesostructured zirconia, but a disordered product was obtained.[10,11] Ying et al.[12] obtained the lamellar and disordered hexagonal structure in the presence of an amphiphilic surfactant and proposed a ligand-assisted templating route. The lamellar and hexagonal mesostructure can also be observed by interaction between long-chain-length primary amine and inorganic species.[13] Using block-copolymer templating, Zhao and co-workers[14,15] demonstrated that very-ordered mesoporous zirconia could be synthesized in nonaqueous solution. They thought that the mesophase could be formed through a mechanism that combines block-copolymer self-assembly with alkylene oxide complexation of the inorganic metal species, whereas Blin et al.[16] proposed that the hydrolysis and polymerization of precursors occurred around surfactant micelles, which resulted in supermicropores formed first and then the supermicropores transformed to mesopores after hydrothermal treatment. Recently, Zhao et al.[17] further developed an "acid−base pair" route to prepare cubic zirconia.

Many properties of nanocrystalline materials are fundamentally different from those of conventional polycrystalline materials, owing to the extremely small crystallite dimension.[18,19] They exhibit increased strength or hardness, improved ductility or toughness, enhanced diffusivity, and increased edges and corners, which all contribute to favorable properties for use in catalysis, electronics, and ceramics. This is why nanocrystalline zirconia has attracted much research attention in the last two decades.[20−23] Though various nanosized or mesoporous metal oxides have successfully been exploited, there are few reports on mesostructured materials with nanocrystalline walls or nanocrystallites. These materials should have more advantages over those materials having only nanocrystalline or ordered mesoporous structures.

For mesostructured or nanocrystalline zirconia, thermal stability is always a challenging area. Many researchers have attempted to improve the thermal stability of these materials. For example, sulfate or phosphate anions are incorporated into the framework to enhance the stability of the mesostructure framework.[12,24−25] Aliovalent and tetravalent dopants, such as Na^{+}, Ca^{2+}, Y^{3+}, Si^{4+}, Ce,[4] Th^{4+}, and so forth, have been used to reinforce the nanocrystalline structures.[26−30] The stabilization was believed to be achieved by strong surface interaction between dopant ions and zirconia or by higher coordination number via the addition of large-size dopants.

In this work, for the first time, nanocrystalline zirconia with the MSU mesostructure was synthesized using a block-copolymer surfactant as the structure-directing agent via a novel solid-state reaction route. To improve the thermal stability of the mesostructure, laponite was introduced into the inorganic framework. The study demonstrates that this novel synthesis methodology is also promising for synthesizing other mesoporous metal oxides and that laponite is a good stabilizer for the mesostructure.

Experimental Section

Chemicals. Block copolymer $HO(CH_2CH_2O)_x(CH_2CH(CH_3)O)_y(CH_2CH_2O)_xH$ (fw = 5800) and zirconyl chloride ($ZrOCl_2 \cdot 8H_2O$) were obtained from Aldrich and used as received. Laponite ($Na_{0.7}$ $[(Si_8Mg_{5.5}Li_{0.3})$ O_{20} $(OH)_4]^{0.7}$) was supplied by Fernz Specialty Chemicals, Australia.

* Corresponding author. E-mail: maxlu@cheque.uq.edu.au. Tel: +61-7-33653885. Fax: +61-7-33656074.
† University of Petroleum.
‡ University of Queensland.

10.1021/jp048190d CCC: $27.50
Published on Web 09/01/2004

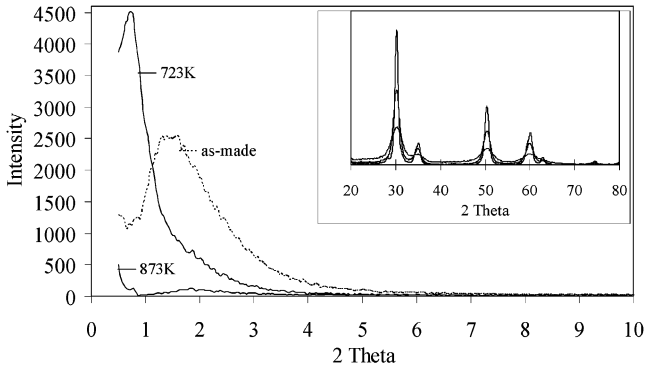

Figure 1. XRD patterns of zirconia samples. (Inset) High-angle peak.

Synthesis. In a typical synthesis, 12.8 g of zirconyl chloride and a certain amount of block-copolymer surfactant were milled together in a mortar and then reacted with 6.4 g of milled sodium hydroxide under vigorous stirring. The resulting product was transferred to an autoclave to crystallize. The crystallizing time and temperature varies for the different inorganic system. After crystallization, the product was washed with deionized water until it was free of Cl^- ions and then washed with ethanol twice to remove water; the surfactant remained in the solid. Finally, the samples were dried at 383 K overnight and calcined at 450 and 600 °C.

The method to prepare the stabilized samples is similar to that above. The only difference is that a certain amount of laponite was milled together with zirconyl chloride and the block copolymer and then reacted with the alkali. Crystalline water in the zirconyl chloride and hygroscopic water during the milling of sodium hydroxide contribute to the micellization process of the surfactant. This methodology can also be applicable to other salt systems for nanocrystalline metal oxide synthesis.

Characterization. Nitrogen adsorption and desorption isotherms at 77.3 K were carried out with Autosorb-1C (Quantachrome, USA) after degassing at 200 °C for 10 h. The mesopore size distribution was calculated from the desorption branch of the isotherms. Low-angle and wide-angle X-ray powder diffraction (XRD) patterns were obtained with a Bruker Axs (Germany) diffractometer using Co Kα radiation with a tube voltage of 40 kV and a tube current of 20 mA. Transmission electron microscopy (TEM) images were taken using a Philips CM200 microscope in bright-field transmission mode. The samples for TEM were prepared by directly dispersing the zirconia particles treated by ultrasonic dispersion onto holey carbon grids. Energy-disperse X-ray (EDX) spectra were taken on a Gatan detector connected to the electron microscope. Scanning electron microscopy (SEM) examinations were performed on a JEOL 6400.

Results and Discussion

The powder XRD patterns of as-synthesized and calcined zirconia are shown in Figure 1. The broader primary low-angle peak is observed in the as-synthesized sample, which is indicative of MSU mesostructure, as also confirmed by the TEM images (Figure 6). The inorganic framework is periodic because it consists of nanocrystallites in the tetragonal phase according to the XRD peaks at high angles. The crystallite size calculated by the Scherrer equation is around 1.5 nm. Upon calcination at 723 K, the intensity of the low-angle XRD peak is substantially greater than that of the as-synthesized sample, suggesting that the mesostructure was retained. The broadening of diffraction is thought to arise from a lack of long-range crystallographic order or finite-size effects.[31] The TEM image (Figure 6) demonstrates that the broadened diffraction here is attributed to the particle-size effect because there are sharp lines for the calcined sample whose size is increased to 6.0 nm. The mesostructure tends to be less ordered after calcination at 873 K because the low-angle peak almost disappeared and the high-angle lines become narrower and sharper. This shows that the crystallization of the inorganic wall during the calcination process resulted in a more disordered mesostructure. We note that the particle was still nanocrystalline and the lattice structure was more ordered upon further crystallizing at higher calcination temperatures, which is confirmed by TEM examination.[32]

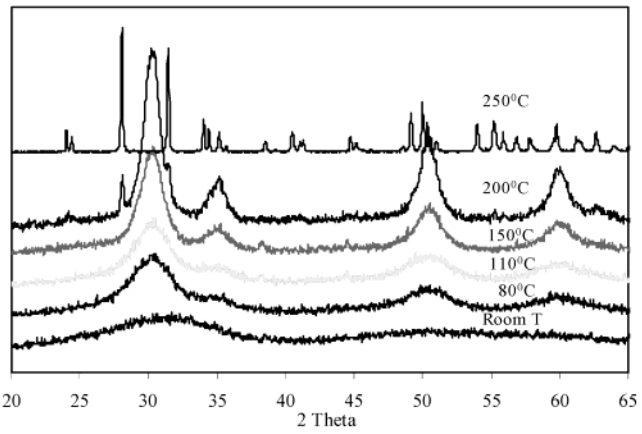

Figure 2. Effect of crystallization temperature on the crystal phases of zirconia.

The nanocrystallite size and mesopore structure can be tailored by varying the crystallization temperature.[33] It can be seen from Figure 2 that the crystallite size increased with the increase in crystallization temperature and that the phase is transformed from tetragonal to monoclinic. The tetragonal phase (t phase) is stable up to 200 °C with some monoclinic phase (m phase). Beyond this temperature, transformation of the t phase into the m phase starts, and at 250 °C, complete transformation occurs. The nanocrystalline sizes at these temperatures are 5.0 and 54.2 nm, respectively. This confirms the previous conclusion that the stability of tetragonal ZrO_2 is due to nanocrystallite size.[34−36] The crystal growth with increasing crystallization temperature is faster and results in larger nanocrystallites.

Nitrogen adsorption/desorption isotherms (Figure 3) indicate that the isotherms of mesoporous zirconia synthesized at different crystallization temperatures are typically IV type with large hysteresis loops except for the sample prepared at 250 °C, which means that the materials obtained with the solid-state reaction using block copolymers as structure-directing agents have mesoporous structure. The capillary condensation partial pressure and the size of the hysteresis loop increases with temperature. This indicates that the pore size is enlarged, which is evidenced by the mesopore distribution shown in Figure 3b. From Figure 3b, we can also see that the mesopore of zirconia prepared with this novel method possesses a monomodal mesopore distribution. The mesoporous diameter can be tuned in the range of 3.8−12.0 nm, and the pore volume increases with temperature before 150 °C. However, nonporous, monoclinic-phase zirconia can be obtained at 250 °C, which testifies to the fact that the mesostructure is destroyed by the phase transformation.[37] The increased pore size at higher crystallization temperature is attributed to the increase in aggregation of micelles. For the PEO-block-PPO surfactant, the hydrophobic capacity is relatively enhanced because the affinity between the hydrophilic groups and water is weakened at higher

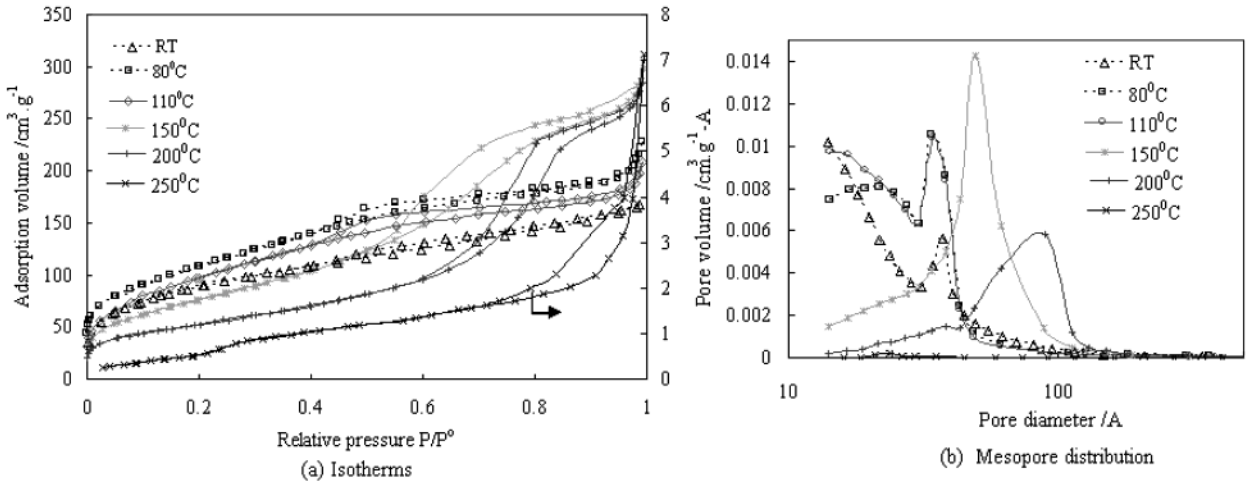

Figure 3. Effect of crystallization temperature on the isotherms and mesopore distribution of nanocrystalline zirconia.

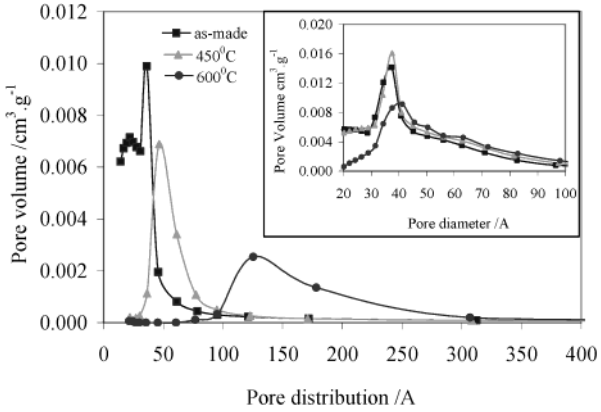

Figure 4. Mesopore-size distribution of zirconia calcined at different temperatures. (Inset) Pore-size distribution of samples stabilized by laponite.

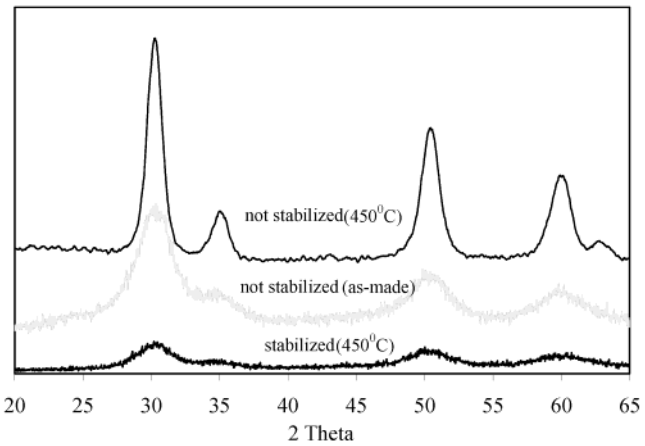

Figure 5. XRD pattern of calcined zirconia before and after stabilization.

temperatures. To decrease the entropy and free energy of the water−organic system, the aggregation number of micelles is increased, which results in the zirconia sample with larger nanocrystallites, thus leading to products with larger mesopores.

The above results show that nanocrystalline zirconia with MSU mesostructure can be obtained using the solid-state reaction route. However, the surface area (Table 1) is dramatically reduced at higher calcination temperatures. In addition, the spread of pore-size distribution (Figure 4) tends to be larger, and the average pore size also shifts to larger values. It is therefore important to improve the structural stability further upon calcination. When incorporating laponite into the synthesis, the mesopore distribution is stabilized by an 0.88% molar ratio of laponite (Figure 4, inset). The results show that the presence of laponite not only enhances the stability of mesostructure but also increases the mesopore volume. The pore-size distribution is almost the same after calcination at 450 °C, and the pore diameter increases very little for the sample calcined at 600 °C. It is worthy to note that the addition of laponite led to narrower pore distribution compared to that of the pure zirconia. The data in Table 1 indicate that the surface area and pore volume can also be retained compared to the data for the as-made sample after it was calcined at 450 °C. Overall, the N_2 adsorption/desorption results showed that laponite is a better stabilizer than other dopants previously reported in the literature.

The XRD patterns shown in Figure 5 demonstrate that laponite can also resist the crystallization of the inorganic framework and inhibits the growth of nanocrystallites. The diffraction peaks of the calcined, stabilized sample are more broadened than the as-made pure zirconia. This means that laponite must have been incorporated into the zirconia framework and formed a strong interaction with Zr^{4+}. This interaction inhibits crystal growth during crystallization in the calcination process; consequently, it forms more fine nanocrystallites, which leads to high surface area. This result is also confirmed by the TEM images shown in Figure 6.

The evidence for disordered, hexagonal-like packing of channels in MSU mesostructures is also evident in the TEM images. The micrograph shows that the nanocrystallites of zirconia formed around the wormholelike pores are regular in diameter although lacking long-range packing order. These short channels and nanocrystallite size are conducive to high activity and conductivity in catalytic and electrode materials, respectively, because of less resistance to mass transport and the charge-transfer process. From Figure 6, it can be seen that the nanocrystallite size of the stabilized samples is much smaller than that of the pure zirconia, particularly for calcined samples. The crystal EDX fringes are shown in Figure 6c. It is observed that for stabilized samples calcined at 600 °C there are merely nanocrystallites about 2.0 nm in size. These results further confirm that the laponite in the inorganic framework played a role in inhibiting crystal growth.

The TEM studies of the pure zirconia calcined at 450 °C showed an apparently mesoporous structure with pores about 6.2 nm in diameter, which corresponds to the value of 6.1 nm calculated by the BJH method. Interestingly, the mesostructure of the laponite-stabilized samples looks more ordered than that

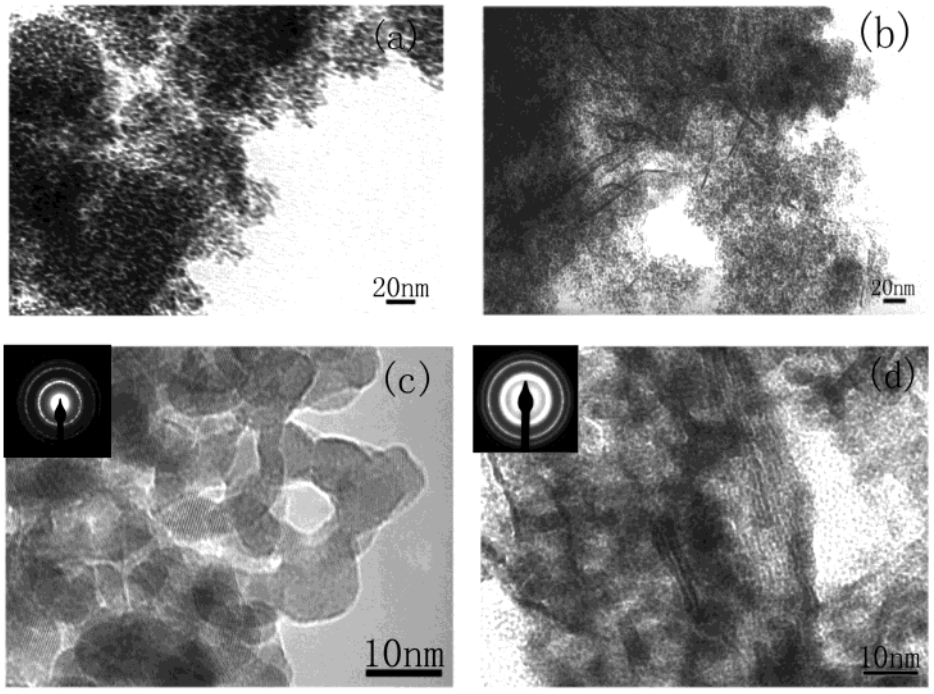

Figure 6. TEM images of pure and stabilized zirconia before and after calcination: (a) pure zirconia as-made, (b) zirconia stabilized by 0.88% laponite, (c) pure zirconia calcined at 450 °C, and (d) zironia stabilized with 0.88% laponite calcined at 600 °C.

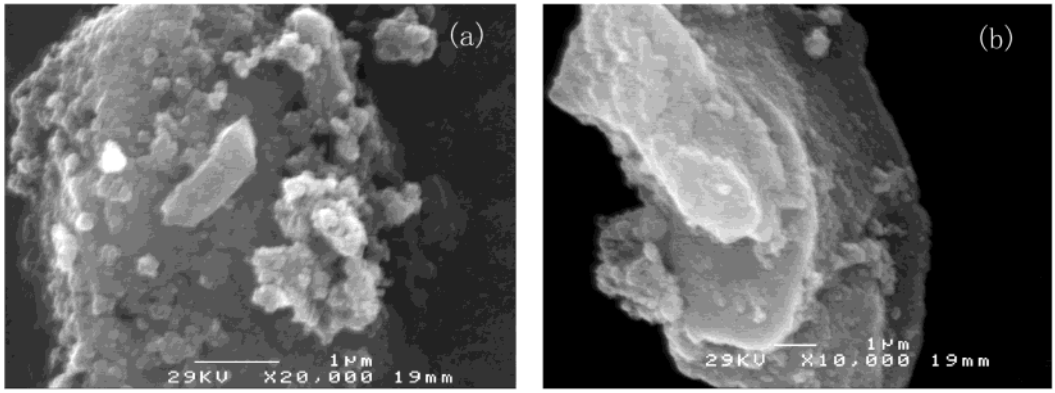

Figure 7. SEM images for as-made zirconia: (a) pure zirconia and (b) stabilized zirconia.

TABLE 1: Effect of Laponite Stabilization on the Surface Area and Pore Structure of Zirconia

	not stabilized			stabilized		
sample	as-made	450 °C	600 °C	as-made	450 °C	600 °C
BET/$m^2\ g^{-1}$	354.2	103.3	51.19	356.5	360.9	231.2
pore volume/$cm^3\ g^{-1}$	0.366	0.279	0.335	0.454	0.472	0.411
pore size/Å	45.8	61.2	178.0	40.8	41.0	45.6

in the pure zirconia. The local lamellar structure can be observed in the mesostructure of the calcined sample. This could be attributed to the interaction between the precursor of zirconia and the inorganic species in laponite. This interaction is achieved via hydrogen bonding between the PEO segments and various inorganic species and may be extended along the direction of the laponite-platelet layer. The Zr−O−Mg−O−Si network is formed upon the condensation of the inorganic pore wall at high temperature, which is the reason that the mesostructure of the calcined laponite-stabilized sample is more ordered. The more ordered mesostructure can be also observed in the SEM images shown in Figure 7. The morphology of the stabilized sample possesses a similar lamellar structure, whereas for pure zirconia, only a disordered structure is observed.

The above discussion demonstrates that the introduction of laponite strongly affects the stability of nanocrystalline zirconia with MSU mesostructure. It is necessary to investigate the optimum amount of laponite that can be incorporated into the mesostructure. The mesopore distributions of zirconia calicined at 450 °C for various amounts of laponite are shown in Figure 8. It is seen that the samples all possess a monomodal pore-size distribution centered around 3.6 nm when the laponite addition is less than 0.88% (molar ratio). For higher amounts (>0.88%) of laponite, a bimodal mesopore distribution is observed. Table 2 shows that the pore volume is drastically increased with the increase in the amount of laponite added, whereas the crystallite size is decreased. The sample that is stabilized by 0.88% laponite exhibits the highest surface area. The optimal amount of laponite addition in nanocrystalline zirconia can be said to be around 0.88%.

The solid-state reaction method using a block copolymer as the structure-directing agent to synthesize nanocrystalline zir-

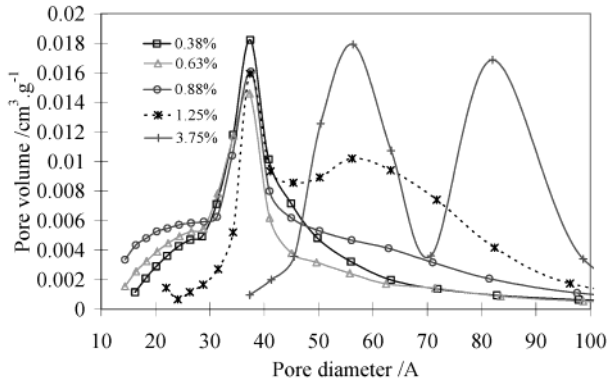

Figure 8. Effect of the amount of laponite on the mesopore distribution of zirconia calcined at 723 K.

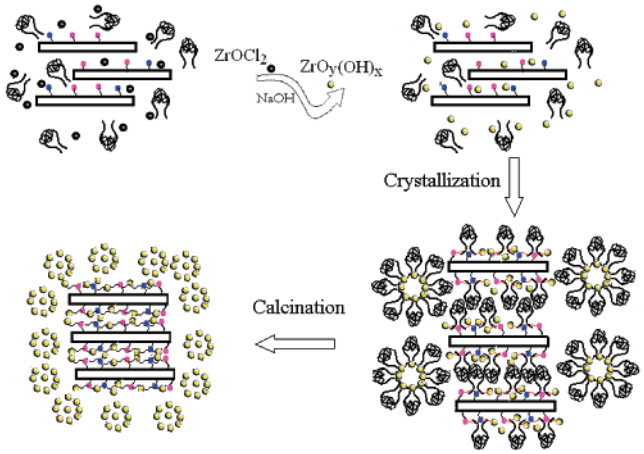

Figure 9. Schematic of the solid-state reaction route involving laponite as the stabilization agent for nanocrystalline zirconia formation.

TABLE 2: Effect of Laponite on the Mesostructure of Zirconia Calained at 450 °C

sample	nanocrystallite size/nm	BET /m^2 g^{-1}	pore volume /cm^3 g^{-1}	pore diameter /Å
Zr−lap-0.38%	2.7	287.9	0.383	40.8
Zr−lap-0.63%	2.1	282.2	0.334	41.0
Zr−lap-0.88%	2.0	360.9	0.472	41.0
Zr−lap-1.25%	1.8	309.7	0.582	41.2, 58.0
Zr−lap-3.75%	1.5	276.2	0.914	63.4, 98.7

conia with MSU mesostructure is the first attempt in this area. Pure zirconia without the addition of a stabilizer can be obtained with a high surface area and a nanocrystallite pore wall. The MSU mesostructure with a nanocrystalline pore wall is periodic in lattice structure, and the pore diameter can be easily tailored by synthesis conditions. This MSU mesostructure with nanocrystalline walls prevents the mesostructure from collapsing.[14,15] However, the structure becomes more disordered and the surface area decreased dramatically at high calcination temperature (>600 °C). To apply this material to high-temperature applications such as solid-oxide fuel cells, we used laponite to improve its stability. The main composition of laponite is SiO_2 and MgO. SiO_2 and MgO can play a stabilization role for the zirconia mesostructure according to their electronic properties and charge sizes. The presence of laponite platelets induces the more ordered and more stable mesostructure. The analogous lamellar structure can also be observed in this mesostructure, particularly in the calcined sample. Laponite can be considered to be a hard template as well. As illustrated in Figure 9, the mechanism of the stabilization of the mesostructure by laponite is proposed as follows.

The zirconia precursors interact strongly with the platelets of laponite via the bridge of PEO segments with hydrogen bonding. Thus, Zr−O−Mg−O−Si networks can form upon the condensation of the framework during the calcination process. In addition, the interaction among various inorganic species can be extended along the direction of the laponite platelet layer. This is the reason that local lamellar structures can be observed in the zirconia mesostructure. The Zr−O−Mg−O−Si networks with large covalent bonds induce stronger interactions for the framework. It is believed that the introduction of laponite not only renders the lamellar structure but also forms the solid mesoporous skeleton. It is the large covalent-bond network that contributes higher stability to the mesostructure. With the increase in laponite amount, the interaction among the inorganic species results in the larger pillared particles, which induce the larger mesopore size and broaden the pore-size distribution. We also found that there is an optimum amount of laponite as a hard template to stabilize the mesostructure and to achieve maximum porosity.

The formation of the MSU mesostructure should be attributed to the cooperative self-assembly of the block-copolymer surfactant with the inorganic species. For the nonionic surfactant, the shape of the micelles changes in the sequence of spherical to hexagonal to lamellar to reverse hexagonal as the concentration increases. In a solid-state reaction, the mass concentration of the surfactant is higher than 70% under all synthesis conditions used because the solvent is supplied only by the crystalline water in zirconyl chloride and a small amount of hydroscopic adsorbed water during milling. This means that the aggregation of the structure-directing agent is similar to the high surfactant concentration situation in aqueous synthesis systems. Thus, the lamellar and reverse hexagonal structures in the micelles are favored. In this unique synthesis system, according to the studies in this work, the mesophase of inorganic and organic templates is most likely to be of the reverse hexagonal structure. The N_2 adsorption/desorption data also showed that the pore diameter of the ziconia samples thus formed is independent of the chain length of the polymer surfactant but depends on the size of the hydrophobic head. This is more evidence confirming the existence of the reverse-hexagonal mesophase.

Conclusions

Nanocrystalline zirconia with MSU mesostructure is synthesized via a novel solid-state reaction route using a block copolymer as the structure-directing agent. Laponite as a hard template and stablizer for the mesostructure has proved to be very effective in tailoring the nanocrystallite size and thermal stability of the zirconia product. The addition of laponite inhibits the crystallization of the zirconia precursor and induces the formation of the more ordered mesostructure. In this novel solid-state synthesis system, the reverse-hexagonal mesophase can be formed, which leads to the MSU mesostructure. In addition, using this novel route, the surface area and pore structure of zirconia can be easily tuned by the synthesis conditions. This methodology using a solid-state reaction could be applied to the synthesis of other metal oxides with high crystallinity and mesostructure stability. Because it is a simple process, the cost for the final-product zirconia is expected to be lower than that of the aqueous routes.

Acknowledgment. Financial support from the Australian Research Council is gratefully acknowledged. We thank Dr. J. Riches and Ms. A. Yago for their assistance on TEM and XRD analysis.

References and Notes

(1) Su, C. L.; Li, J. R.; He, D. H. *Appl. Catal. A* **2000**, *202*, 81.
(2) Wong M. S.; Antonelli, D. M.; Ying J. Y. *Nanostruct. Mater.* **1997**, *9*, 165.
(3) Wu Z. G.; Zhao Y. X.; Liu D. S. *Microporous Mesoporous Mater.* **2004**, *68*, 127.
(4) Mamak, M.; Coombs, N.; Ozin, G. *J. Am. Chem. Soc.* **2000**, *122*, *8932*.
(5) Verveij, H. *Adv. Mater.* **1998**, *10*, 1483.
(6) Ziehfreund, A.; Simon, U.; Maier, W. F. *Adv. Mater.* **1996**, *8*, 424.
(7) van Berkel, F. P. F.; van Heuveln, F. H.; Huijsmans, J. P. P. *Solid State Ionics* **1994**, *72*, 240.
(8) Knowles, J. A.; Hudson, M. J. *J. Chem. Soc., Chem. Commun.* **1995**, *20*, 2083.
(9) Trens, P.; Hudson, M. J.; Denoyel, R. *J. Mater. Chem.* **1998**, *8*, 2147.
(10) Pacheco, G.; Zhao, E.; Garcia, A.; Sklyarov, A.; Fripiat, J. J. *J. Mater. Chem.* **1998**, *8*, 219.
(11) Zhao, E.; Hernandez, O.; Pacheco, G.; Hardcastle, S.; Fripiat, J. J. *J. Mater. Chem.* **1998**, *8*, 1635.
(12) Wong, M. S.; Ying, J. Y. *Chem. Mater.* **1998**, *10*, 2067.
(13) Reddy, J. S.; Sayari, A. *Catal. Lett.* **1996**, *38*, 219.
(14) Yang, P. D.; Zhao, D. Y.; Margolese, D. I.; Chmelka, B. F.; Stucky, G. D. *Nature* **1998**, *396*, 152.
(15) Yang, P. D.; Zhao, D. Y.; Margolese, D. I.; Chmelka, B. F.; Stucky, G. D. *Chem. Mater.* **1999**, *11*, 2813.
(16) Blin, J. L.; Flamant, R.; Su, B. L. *Int. J. Inorg. Mater.* **2001**, *3*, 959.
(17) Tian, B. Z.; Liu, X. Y.; Tu, B.; Yu, C. Z.; Fan, J.; Wang, L. M.; Xie, S. H.; Stucky, G. D.; Zhao, D. Y. *Nat. Mater.* **2003**, *2*, 159.
(18) Lu, K. *Mater. Sci. Eng.* **1996**, *16*, 161.
(19) Ajayan, P. M.; Schadler, L. S.; Braun, P. V. *Nanocomposite Science and Nanotechnology*; Wiley-VCH: Weinheim, Germany, 2003; Chapters 1 and 17.
(20) Panda, A. B.; Roy, J. C.; Pramanik, P. *J. Eur. Ceram. Soc.* **2003**, *23*, 3043.
(21) Feng, X.; Bai, Y. J.; Lu, B.; Zhao, Y. R.; Yang, J.; Chi, J. R. *J. Cryst. Growth* **2004**, *262*, 420.
(22) Kolen'ko, Yu. V.; Maximov, V. D.; Burukhin, A. A.; Muhanov, V. A.; Churagulov, B. R. *Mater. Sci. Eng., C* **2003**, *23*, 1033.
(23) Noh, H. J.; Seo, D. S.; Kim, H.; Lee, J. K. *Mater. Lett.* **2003**, *57*, 2425.
(24) Shen, S. D.; Tian, B. Z.; Yu, C. Z.; Xie, S. H.; Zhang, Z. D.; Tu, B.; Zhao, D. Y. *Chem. Mater.* **2003**, *15*, 4046.
(25) Sominski, E.; Gedanken, A.; Perkas, N.; Buchkremer, H. P.; Menzler, N. H.; Zhang, L. Z.; Yu, J. C. *Microporous Mesoporous Mater.* **2003**, *60*, 91.
(26) Ho, S. M. *Mater. Sci. Eng.* **1982**, *54*, 23.
(27) Benedetti, A.; Fagherazzi, G.; Pinna, F. *J. Am. Ceram. Soc.* **1989**, *72*, 467.
(28) Del, M. F.; Larsen, W.; Mackenzie, J. D. *J. Am. Ceram. Soc.* **2000**, *83*, 628.
(29) Zhou, E.; Bhaduri, S.; Bhaduri, S. B.; Lewis, I. R.; Griffiths, P. R. *Miner., Met. Mater. Soc., Electron., Magn. Photonic Mater. Div. Monogr. Series* **1996**, 123.
(30) Chen Li, I.-W.; Penner-Hahn, J. E. *J. Am. Ceram. Soc.* **1994**, *77*, 118.
(31) Bagshaw, S. A.; Prouzet, E.; Pinnavaia, T. J. *Science* **1995**, *269*, 1242.
(32) Liu, X. M.; Yan, Z. F.; Lu, G. Q. *Chin. Sci. Bull.* **2004**, *49*, 975.
(33) Liu, X. M.; Lu, G. Q.; Yan, Z. F. *Stud. Surf. Sci. Catal.* **2003**, *146*, 239.
(34) Garvie, R. G. *J. Phys. Chem.* **1978**, *82*, 218.
(35) Chatterjee, A.; Pradhan, S. K.; Dakka, A.; De, M.; Chakravorthy, D. *J. Mater. Res.* **1996**, *9*, 263.
(36) Aita, C. R.; Wiggins, M. D.; Whig, R.; Scanlan, C. M.; Gajdardziska-Josifovska, M. *J. Appl. Phys.* **1994**, *79*, 1176.
(37) Huang, Y. Y.; McCarthy, T. J.; Sachtler, W. M. H. *Appl. Catal.* **1996**, *148*, 135.